



Published in final edited form as:

Science. 2013 June 7; 340(6137): . doi:10.1126/science.1232806.

Geniculocortical Input Drives Genetic Distinctions Between Primary and Higher-Order Visual Areas

Shen-Ju Chou^{1,*†}, Zoila Babot^{1,*}, Axel Leingärtner^{1,‡}, Michele Studer^{2,§}, Yasushi Nakagawa^{1,||}, and Dennis D. M. O'Leary^{1,¶}

¹Molecular Neurobiology Laboratory, The Salk Institute for Biological Studies, La Jolla, CA, USA

²Institute of Biology Valrose, INSERM, Nice, France

Abstract

Studies of area patterning of the neocortex have focused on primary areas, concluding that the primary visual area, V1, is specified by transcription factors (TFs) expressed by progenitors. Mechanisms that determine higher-order visual areas (V^{HO}) and distinguish them from V1 are unknown. We demonstrated a requirement for thalamocortical axon (TCA) input by genetically deleting geniculocortical TCAs and showed that they drive differentiation of patterned gene expression that distinguishes V1 and V^{HO} . Our findings suggest a multistage process for area patterning: TFs expressed by progenitors specify an occipital visual cortical field that differentiates into V1 and V^{HO} ; this latter phase requires geniculocortical TCA input to the nascent V1 that determines genetic distinctions between V1 and V^{HO} for all layers and ultimately determines their area-specific functional properties.

The neocortex is patterned into functionally distinct fields that include primary sensory areas, which receive modality-specific sensory input from thalamocortical axons (TCAs) that originate from the principal sensory nuclei of the dorsal thalamus (dTh), and higher-order sensory areas that are connected with the primary areas through intracortical projections (1). Studies of mechanisms that pattern the neocortex into areas, known as arealization, have focused on primary areas and have led to the prevailing model that genetic mechanisms intrinsic to the neocortex are predominant in arealization (2). Transcription factors (TFs) expressed in neocortical progenitors determine the size and position of primary areas (2–5) and regulate guidance information that governs the area-specific targeting of TCAs (6). However, roles for TCAs in arealization remain vague (7–10), and important features of arealization, such as differential gene expression in the embryonic neocortex that relates to nascent areas, develop independently of TCA input (9, 10).

¶Corresponding author. doleary@salk.edu.

*These authors contributed equally to this work.

†Present address: Institute of Cellular and Organismic Biology, Academia Sinica, Taipei, Taiwan.

‡Present address: University Cancer Center Hamburg, University Medical Center Hamburg-Eppendorf, Hamburg, Germany.

§Present address: Institute of Biology Valrose, iBV, UMR INSERM1091/CNRS7277/UNS, Nice, F-06108, France; and University of Nice Sophia-Antipolis, UFR Sciences, Nice, F-06108, France.

||Present address: Department of Neuroscience, Stem Cell Institute and Developmental Biology Center, University of Minnesota, Minneapolis, MN 55455, USA.

Supplementary Materials

www.sciencemag.org/cgi/content/full/340/6137/1239/DC1

Materials and Methods

Figs. S1 to S9

References (28–31)

Higher-order areas outnumber primary areas by roughly 10-fold; for example, in mouse, nine higher-order visual areas (V^{HO}) are positioned around the primary visual area (V1) within the occipital neocortex (11). However, mechanisms that specify and regulate differentiation of the particular properties of higher-order areas and distinguish them from primary areas have yet to be explored (11, 12). To perform genetic manipulations of dTh neurons required for these studies, we created $ROR\alpha$ -IRES-Cre mice ($ROR\alpha^{Cre}$; fig. S1, A and B) with $ROR\alpha$ function intact and expression of Cre recombinase driven by $ROR\alpha$ regulatory elements (13). Crossing this $ROR\alpha^{Cre}$ mouse to conditional reporter lines (fig. S1) revealed Cre-mediated recombination in neurons of the principal sensory nuclei in dTh at embryonic day 14.5 (E14.5), shortly after they become postmitotic (14), with robust recombination in the dorsal lateral geniculate nucleus (dLG) (fig. S1, C to K), which forms the geniculocortical TCA projection that relays visual information from the eyes selectively to V1. Little or no recombination was detected in the neocortex through the end of the first postnatal week, encompassing the differentiation of cortical areas and the time frame of our study (fig. S1, C to K).

We crossed $ROR\alpha^{Cre}$ mice to mice in which the third exon of the COUP-TF1 gene is flanked by loxP sites, i.e. floxed (fl) COUP-TF1 [$COUP-TF1^{fl/fl}$ is described in (5)], because COUP-TF1 is strongly expressed in dLG, COUP-TF1 deletion diminishes axon growth (15), and most TCAs fail to reach the cortex in COUP-TF1-null mice (16). COUP-TF1-null mice are not useful for our studies because of viability issues and defects in cortical development (16). In contrast, the conditional knockout (cKO) mice ($ROR\alpha^{Cre/+}$ or $ROR\alpha^{Cre/Cre}$; $COUP-TF1^{fl/fl}$) were viable and retained robust COUP-TF1 expression in the neocortex (fig. S2, A and B), but COUP-TF1 was deleted from dLG by E15.5 (fig. S2, A and B), and dLG size in cKO mice progressively decreased from the wild-type (WT) size embryonically to virtually absent by postnatal day 7 (P7) (figs. S2, C and D, and S3).

To visualize TCA projections in the cortex, we first used serotonin [5-hydroxytryptamine (5-HT)] immunostaining on tangential sections of flattened P7 cortices. In P7 WT mice, 5-HT staining revealed the geniculocortical TCA projection from dLG to V1, as well as TCA projections from the ventroposterior nucleus (VP) to the primary somatosensory area (S1) and from the medial geniculate nucleus (MG) to the primary auditory area (A1) (Fig. 1A). In P7 cKO mice, 5-HT staining showed that TCA projections to S1 and A1 were intact, but the geniculocortical TCA projection to V1 was absent (Fig. 1A). The loss of geniculocortical input to V1 in P7 cKO mice was confirmed by anterograde and retrograde axon tracing from dLG and V1 (fig. S4, A and B) and by crossing the cKO mice to a ROSA26-GAP43-eGFP reporter line that labels TCAs by $ROR\alpha^{Cre}$ reporter activation (fig. S5A). Thus, conditional deletion of COUP-TF1 from dLG using the $ROR\alpha^{Cre}$ line resulted in deletion of the geniculocortical TCA projection by P7, but COUP-TF1 remained intact in the cortex.

To determine the time course of the geniculo-cortical TCA projection in cKO mice as compared to WT mice, we bred $ROR\alpha^{Cre}$ mice on either a WT ($COUP-TF1^{fl/+}$; $ROR\alpha^{Cre/+}$) or cKO ($COUP-TF1^{fl/fl}$; $ROR\alpha^{Cre/+}$ or $COUP-TF1^{fl/fl}$; $ROR\alpha^{Cre/Cre}$) background, to a conditional reporter line (Ai14 tdTomato) (17). Activation of the tdTomato reporter with the $ROR\alpha^{Cre}$ line labeled, at high resolution, geniculocortical TCAs from the dLG and TCAs from VP and MG projecting to S1 and A1 (Fig. 1B). Geniculocortical TCAs extend tangentially in the subplate and underlie the cortical plate (CP) of nascent V1 by E16.5, invade after birth the overlying V1 CP, and over the first postnatal week arborize in V1 layer 4, their predominant target layer (18). At E16.5, before TCAs invade the CP, the appearance of tdTomato-labeled TCAs was indistinguishable between WT and cKO mice, with a high density of labeled TCAs present in the occipital cortex of both (Fig. 1B). At P1, when geniculocortical TCAs normally invade the CP of V1, the density of labeled axons in the occipital cortex was substantially decreased in cKO mice as compared to WT mice (Fig.

1B). By P3, labeled geniculocortical TCAs were robustly arborizing in layer 4 of V1 of WT mice but were virtually absent from V1 and from the entire occipital cortex of cKO mice (Fig. 1B). These findings were corroborated by retrograde axon tracing from V1 and S1 (figs. S4 and S6). Thus, geniculo-cortical TCAs appeared WT in embryonic cKO mice but were eliminated early postnatally before significantly invading the CP or arborizing in layer 4 of V1.

Retrograde labeling from V1 and S1 showed that the area specificity of TCA input in the cKO mice was similar to that in the WT mice (19, 20) (figs. S4 and S6). Overall size, surface area, and tangential dimensions of the cortex were also similar between WT and cKO mice, as was S1 position in the cortex and occipital cortex size, which in WT mice is primarily V1 and V^{HO} (fig. S5). Other features of the occipital cortex, including thickness, cell density, and lamination, had similar appearances in adult cKO and WT mice (fig. S7). Thus, mechanisms intrinsic to the cortex determine the overall size of the occipital visual cortical field and of S1 relative to it, independent of geniculocortical TCA input.

This cKO line provided a model to address whether geniculocortical TCA input to V1 differentiates the occipital visual cortical field into V1 and V^{HO} and whether its early postnatal deletion disturbs this patterning. The distinct properties and functions that distinguish V1 from V^{HO} are largely determined by their genetic profiles; i.e., differences in their patterned expression of sets of genes. Therefore, we developed gene markers that distinguished V1 and V^{HO} and were exemplary of their distinct genetic profiles. We assessed in WT mice when area patterning is mature, at P7 and later, the expression of candidate genes to identify those that marked V1 or V^{HO} in patterns that distinguished them and fully delineated one or the other, or both uniquely, using tangential sections of flattened cortices and cortical whole mounts, augmented with sagittal sections to also assess laminar expression. The majority of genes expressed in visual areas did not delineate nor distinguish V1 and/or V^{HO}, but we identified a set of genes that did, and by definition they are among those that generate the distinct properties that define and distinguish V1 and V^{HO} (21–27).

Figure 2A illustrates the two types of expression patterns that delineated V1 and 5-HT staining to mark geniculocortical TCAs terminating in layer 4 of V1. In P7 WT mice, ROR β was highly expressed in V1 layer-4 neurons but at low levels in V^{HO}, whereas in P14 WT mice, Igfbp4 expression was not detected in V1 but was robust in layers 2/3 of V^{HO}. The relationship of these expression patterns to geniculocortical TCA input to V1 suggests that this input induces the patterned expression of genes such as ROR β and represses the patterned expression of genes such as Igfbp4. In P7 cKO mice, coincident with loss of geniculocortical TCA input to V1, ROR β expression exhibited a significant reduction in V1, complemented by a significant increase of ROR β expression in V^{HO}, whereas Igfbp4 expression exhibited a strong up-regulation in V1 of P14 cKO mice (Fig. 2A). We performed densitometry of ROR β expression to quantify its areal expression in P7 WT and cKO mice (Fig. 2B). In P7 WT mice, V1 and S1 had similar high levels of ROR β expression and significantly lower expression in V^{HO}, resulting in a trough in expression intensity coincident with V^{HO} (Fig. 2C). In P7 cKO mice, S1 had high expression similar to that in WT mice, but the high expression in V1 and the low expression trough coincident with V^{HO} were replaced by flattened ROR β expression across the occipital visual cortical field of V^{HO} and V1. The absence in cKO mice of ROR β expression differences between V^{HO} and V1 characteristic of WT mice was due to both increased expression in V^{HO} and decreased expression in V1, and unlike WT mice, no significant difference was evident in expression levels between V^{HO} and V1 in the cKO mice (Fig. 2C,D).

Gene markers in our panel suitable for whole-mount in situ hybridization (WMISH) at P7 delineated V1 and V^{HO} in the intact brain, while retaining the natural shapes and positions

of areas. In P7 WT cortices, moderate expression of *Igfbp5* selectively marked the entire V1 and distinguished it from V^{HO} , which had nondetectable levels of *Igfbp5*. In P7 cKO cortices, *Igfbp5* expression in V1 was diminished to a level indistinguishable from that in V^{HO} , and the entire occipital visual cortical field had low or nondetectable *Igfbp5* expression. In P7 WT mice, both *cadherin8* (*Cad8*) and *Lmo4* showed opposing expression patterns as compared to *Igfbp5*, with higher expression in V^{HO} than V1, in distinct patterns that fully delineated V1 and V^{HO} independently. In cKO mice, the patterned expression of *Cad8* and *Lmo4* was lost, and neither distinguished V^{HO} from V1; instead, the occipital visual cortical field exhibited a homogeneous expression across its full extent, due in large part to increased expression of both genes throughout V1 to a level equivalent to that in V^{HO} (Fig. 3).

The expression of the type 2 muscarinic acetylcholine receptor (m2AChR) and distinct phosphorylation forms of neurofilaments (SMI-32) in adult WT mice delineate and distinguish V1 and V^{HO} and contribute to their specific functional properties (11, 26, 27). Immunostaining for m2AChR revealed low or nondetectable labeling of V^{HO} between the strongly labeled V1 and S1 (Fig. 4A). In adult cKO mice, immunostaining for m2AChR was substantially diminished in layer 4 throughout V1, coupled with significantly increased staining of layer 4 in V^{HO} , resulting in homogeneous low staining across the entire occipital visual cortical field normally composed of V1 and V^{HO} (Fig. 4B). In situ hybridization for m2AChR recapitulated both the WT and cKO expression patterns observed with m2AChR staining patterns (Fig. 4B), showing that the changes in the cKO mice reflected a reduction of m2AChR expression by V1 layer 4 neurons rather than the loss of presynaptic m2AChR protein (27). Immunostaining for SMI-32 in adult WT mice also delineated V1 from V^{HO} with robust staining of V1 and low staining of V^{HO} , but with staining predominantly localized to projection neurons in layers 3 and 5. Deletion of geniculocortical TCAs to V1 in the cKO mice produced a substantial reduction in SMI-32 staining of both layer-3 and -5 projection neurons in V1 of adult cKO mice as compared to WT mice, resulting in homogeneous staining of layers 3 and 5 across the occipital visual cortical field and an inability to distinguish V1 from V^{HO} (Fig. 4, A and B).

We have shown a prominent role for TCA input and redefined the role of intrinsic genetic regulation of the differentiation of higher-order sensory areas from primary sensory areas (fig. S8A). We selectively deleted geniculocortical TCA input to V1 early in postnatal development to accomplish two goals: (i) to assess the requirement of geniculocortical TCA input for the differentiation of genetic profiles that distinguish V1 from V^{HO} and establish their specific functional properties; and (ii) to isolate the function of intrinsic genetic mechanisms to assess their role relative to geniculocortical TCAs in the specification and differentiation of V1 and V^{HO} . Isolating in cKO mice the function of intrinsic genetic mechanisms in patterning V1 and V^{HO} redefined their roles in arealization and showed that they specify an occipital visual cortical field that has a similar genetic profile over its extent. Genulocortical TCA input is required postnatally to differentiate the visual cortical field into V1 and V^{HO} and establish the genetic profiles that delineate and distinguish them. Regardless of whether in WT mice the gene and protein markers were more highly expressed in V1 than V^{HO} , or vice versa, they exhibited significant changes in their patterned expression in cKO mice in which geniculocortical TCA input was deleted, resulting in a uniform intermediate level of expression across the occipital visual cortical field that would normally differentiate into V1 and V^{HO} (fig. S8B). The change from patterned to uniform expression occurred through bidirectional changes in expression, with both down-regulation of expression in V1 and up-regulation in V^{HO} , or vice versa, to produce intermediate expression levels across the occipital visual cortical field despite the selective targeting in WT mice of geniculocortical TCAs to only part of the occipital visual cortical field; i.e., the nascent V1. These changes in patterned gene expression occurred not

only in the primary TCA target layer 4, but also in layers 2, 3, and 5, which receive little or no direct TCA input.

Our findings require a revision of the prevailing model of arealization and indicate a working model with distinct stages: Intrinsic genetic mechanisms specify an occipital visual cortical field with a relatively uniform genetic profile, followed by its differentiation into V1 and V^{HO} driven by geniculocortical TCA input targeted selectively to the nascent V1 (fig. S9). This multistage process of arealization creates the hierarchical cortical organization of primary and higher-order visual areas that is required for proper visual perception and behavior.

Supplementary Material

Refer to Web version on PubMed Central for supplementary material.

Acknowledgments

We thank members of the O'Leary lab for discussion, including S. May for developing Igfbp5 as a V1 marker using WMISH, and B. Higgins and H. Gutierrez for maintaining mice. We thank M. Goulding (Salk Institute) for the ROSA-GAP43-eGFP reporter line, K.-F. Lee (Salk Institute) for the *IRES/Cre/FRT/neo/FRT* construct, A. Nagy (Mount Sinai Hospital) for the R1 ES cells, J. Simon (Salk MultiMedia Relations) for help making Adobe Illustrator schematics, and C. Peto (Salk Institute Neuroscience Imaging Core) for help using ImageJ software. Support was provided by NIH R01 grants NS31558 and MH086147 and the Vincent J. Coates Chair of Molecular Neurobiology (D.D.M.O.). M.S. is supported by the ANR "2009 Chaires d'Excellence" Program, France, grant number R09125AA. Z.B. was a recipient of postdoctoral fellowships from the Spanish Ministry of Education and Science and from the Generalitat de Catalunya (Spain).

References and Notes

1. Felleman DJ, Van Essen DC. *Cereb Cortex*. 1991; 1:1. [PubMed: 1822724]
2. O'Leary DD, Chou SJ, Sahara S. *Neuron*. 2007; 56:252. [PubMed: 17964244]
3. Bishop KM, Goudreau G, O'Leary DD. *Science*. 2000; 288:344. [PubMed: 10764649]
4. Hamasaki T, Leingärtner A, Ringstedt T, O'Leary DD. *Neuron*. 2004; 43:359. [PubMed: 15294144]
5. Armentano M, et al. *Nat Neurosci*. 2007; 10:1277. [PubMed: 17828260]
6. Leingärtner A, Richards LJ, Dyck RH, Akazawa C, O'Leary DD. *Cereb Cortex*. 2003; 13:648. [PubMed: 12764041]
7. Rakic P, Suñer I, Williams RW. *Proc Natl Acad Sci USA*. 1991; 88:2083. [PubMed: 2006147]
8. Dehay C, Giroud P, Berland M, Killackey H, Kennedy H. *J Comp Neurol*. 1996; 367:70. [PubMed: 8867284]
9. Miyashita-Lin EM, Hevner R, Wassarman KM, Martinez S, Rubenstein JL. *Science*. 1999; 285:906. [PubMed: 10436162]
10. Nakagawa Y, Johnson JE, O'Leary DD. *J Neurosci*. 1999; 19:10877. [PubMed: 10594069]
11. Wang Q, Burkhalter A. *J Comp Neurol*. 2007; 502:339. [PubMed: 17366604]
12. Marshel JH, Garrett ME, Nauhaus I, Callaway EM. *Neuron*. 2011; 72:1040. [PubMed: 22196338]
13. Nakagawa Y, O'Leary DD. *Dev Neurosci*. 2003; 25:234. [PubMed: 12966220]
14. Lund RD, Mustari MJ. *J Comp Neurol*. 1977; 173:289. [PubMed: 856885]
15. Armentano M, Filosa A, Andolfi G, Studer M. *Development*. 2006; 133:4151. [PubMed: 17021036]
16. Zhou C, et al. *Neuron*. 1999; 24:847. [PubMed: 10624948]
17. Madisen L, et al. *Nat Neurosci*. 2010; 13:133. [PubMed: 20023653]
18. López-Bendito G, Molnár Z. *Nat Rev Neurosci*. 2003; 4:276. [PubMed: 12671644]
19. Bilateral enucleation in marsupials, which leads to decreased dLG size because of loss of retinal input, results in aberrant TCA input to V1 from dTh nuclei that normally project exclusively to other primary areas (20). Despite the selective deletion of the geniculocortical TCA projection in

cKO mice, DiI injections into the putative V1 of the cKO mice did not aberrantly label neurons in VP, MG, or elsewhere in dTh (figs. S4 and S6). Injections of a second, retrograde tracer, DiD, targeted to nascent S1 and distinguishable from DiI injected into nascent V1 of the same mice, labeled a similar-appearing high density of VP neurons in WT and cKO mice at both P0 and P7, and at late embryonic ages, but in neither WT nor cKO mice did S1 injections label neurons in dLG (figs. S4 and S6).

20. Karlen SJ, Kahn DM, Krubitzer L. *Neuroscience*. 2006; 142:843. [PubMed: 16934941]
21. The marker genes identified that met our criteria included those encoding the TFs, Lmo4 and ROR β , and the cell adhesion molecule Cad8, all of which function in cortical development (10, 13, 22–24); insulin-like growth factor–binding proteins Igfbp4 and Igfbp5 (25); and m2AChR and neurofilament subunits with the nonphosphorylated epitope SMI-32 that contribute to functional distinctions between V1 and V^{HO} (11, 26, 27). One subset of marker genes had more robust expression in V1 than V^{HO} (ROR β , Igfbp5, m2AChR, and SMI-32) and the other in V^{HO} than V1 (Igfbp4, Lmo4, and Cad8). Each clearly identified the border between V1 and V^{HO} and was expressed more-or-less uniformly throughout either V1 or V^{HO}.
22. Bulchand S, Subramanian L, Tole S. *Dev Dyn*. 2003; 226:460. [PubMed: 12619132]
23. Kashani AH, et al. *J Neurosci*. 2006; 26:8398. [PubMed: 16899735]
24. Jabaudon D, Shnyder SJ, Tischfield DJ, Galazo MJ, Macklis JD. *Cereb Cortex*. 2012; 22:996. [PubMed: 21799210]
25. Firth SM, Baxter RC. *Endocr Rev*. 2002; 23:824. [PubMed: 12466191]
26. Van der Gucht E, Hof PR, Van Brussel L, Burnat K, Arckens L. *Cereb Cortex*. 2007; 17:2805. [PubMed: 17337746]
27. van der Zee EA, Matsuyama T, Strosberg AD, Traber J, Luiten PGM. *Histochemistry*. 1989; 92:475. [PubMed: 2807994]

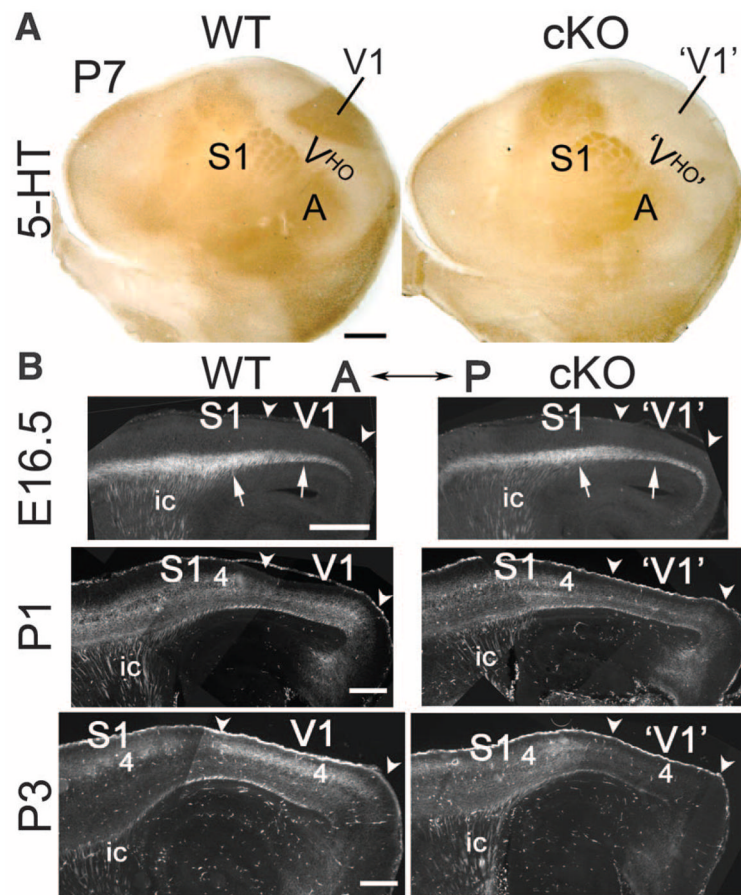


Fig. 1. Selective deletion of geniculocortical TCA projection to V1 in $ROR\alpha$ -IRES-Cre floxed COUP-TF1 cKO mice occurs early postnatally

(A) Geniculocortical projection to V1 is selectively absent in P7 cKO mice. 5-HT immunostaining on tangential sections through layer 4 of P7 WT (COUP-TF1^{fl/+}; $ROR\alpha^{Cre/+}$) and cKO (COUP-TF1^{fl/fl}; $ROR\alpha^{Cre/+}$) flattened cortices is shown. Rostral is at left and medial at the top. 5-HT staining reveals TCA input from principal sensory thalamic nuclei to primary sensory areas: dLG to V1, VP to S1, and MG to the primary auditory area (A). The 5-HT-negative region surrounding V1 is composed of V^{HO}. In P7 cKO mice, 5-HT immuno-stained geniculocortical TCA input to V1 is absent. 5-HT staining of S1 appeared modestly diminished in cKO as compared to WT mice probably because COUP-TF1 may influence TCA input from VP, which expresses Cre (fig. S1) and exhibits COUP-TF1 deletion (fig. S2), but VP is less affected than dLG by COUP-TF1 deletion (figs. S2 and S4 to S6). (B) Time course of the deletion of geniculocortical TCA projection from dLG to V1 revealed in WT (COUP-TF1^{fl/+}; $ROR\alpha^{Cre/+}$; Ai14) and cKO (COUP-TF1^{fl/fl}; $ROR\alpha^{Cre/+}$; Ai14) mice crossed to the Ai14 line with the Cre-inducible axon reporter tdTomato. Sagittal sections from E16.5, P1, and P3 WT and cKO cortices, showing TCAs labeled by tdTomato reporter activated by Cre expressed in dLG and VP (anterior to the left, dorsal at the top) are shown. At E16.5, labeled TCAs (arrows) are densely packed in the subplate underlying the cortical plate of nascent V1, with the TCA projection being indistinguishable between WT and cKO mice. At P1, the geniculocortical TCA projection is beginning to invade the overlying CP of V1 in WT mice but is retarded in the cKO mice. By P3, the geniculocortical TCA projection is densely terminating in V1 of WT mice but is virtually absent from V1 in cKO mice. Abbreviations are as follows: 4, layer 4; ic, internal capsule; arrowheads

approximate the anterior (A) – posterior (P) extent of nascent V1. Scale bars, 0.5 mm in (A) and 0.2 mm in (B).

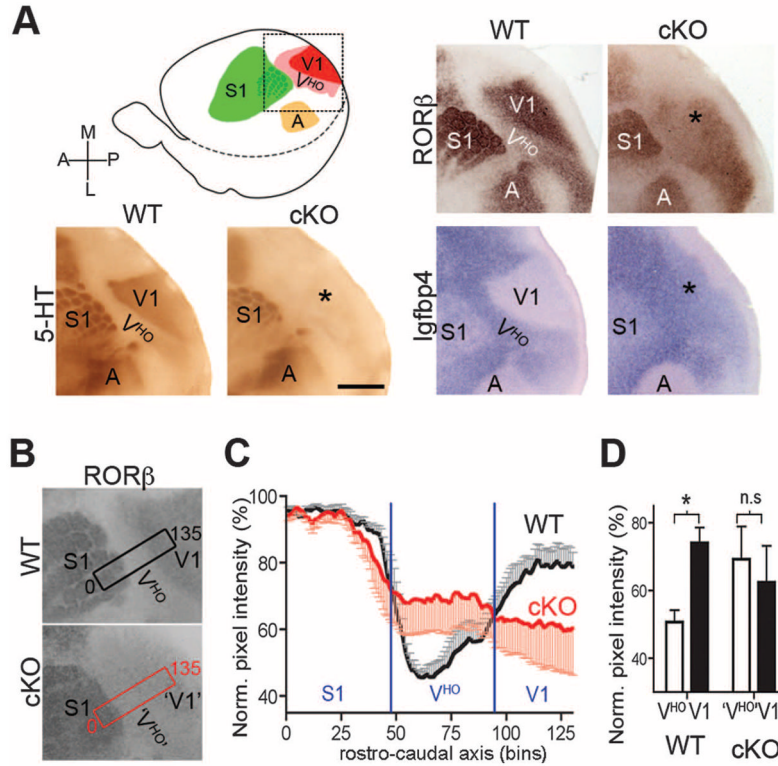


Fig. 2. Differentiation of complementary gene markers that distinguish V1 from V^{HO} requires the postnatal influence of geniculocortical TCA projection
(A) 5-HT immunostained tangential sections of flattened cortices to reveal TCA input and RORβ and Igfbp4 in situ hybridization (ISH) from WT (COUP-TF1^{fl/+}; RORα^{Cre/+}) and cKO (COUP-TF1^{fl/fl}; RORα^{Cre/+}) mice; the field shown is indicated in the schematic. 5-HT and RORβ labeling were performed on sections through layer 4 of P7 cortices; Igfbp4 labeling was done on sections through layers 2/3 of P14 cortices. In WT mice, RORβ is strongly expressed in V1 and low in V^{HO}, whereas Igfbp4 expression is low in V1 and high in V^{HO}. The lack of TCA input in cKO V1 (*) is accompanied by a loss in differential expression patterns of RORβ and Igfbp4 that distinguish V1 from V^{HO} in WT mice. Scale bar, 1 mm. **(B)** RORβ expression at P7 from collapsing all tangential sections through layer 4. The rectangles are 100 μm wide and 2700 μm long and indicate the area used for pixel intensity measurements shown in (C) and (D). **(C)** Plot of the normalized pixel intensity (mean ± SEM) in the rectangular field shown in (B). Each bin is 100 μm wide and 20 μm long and encompasses expression throughout layer 4 (z axis). The expression of RORβ in barrel B1 in the posterior medial barrel subfield of S1 is set at 100; other data are normalized to it. In WT (black, n = 4) mice, the RORβ expression is high in S1 and V1 and low in V^{HO}, whereas in cKO mice (red, n = 4), expression is flattened across the occipital visual cortical field due to up-regulation in V^{HO} and down-regulation in V1. **(D)** Bar graph of the statistical analysis performed with data from (C). Significant difference in RORβ expression intensity between V^{HO} (white) and V1 (black) was observed in WT mice (*P < 0.0001), but not in cKO mice (n.s., not significant).

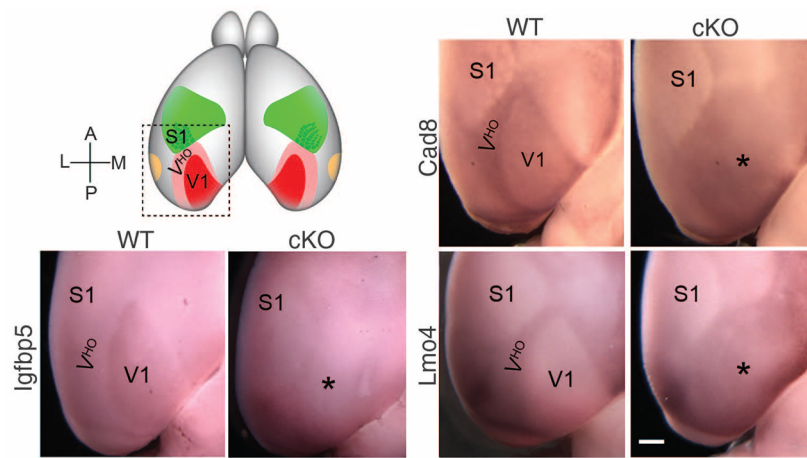


Fig. 3. V1 and V^{HO} delineated by complementary gene expression patterns are replaced with a uniform occipital visual cortical field after deletion of geniculo-cortical TCA input

Photos show the posterior part of P7 WT (COUP-TF1^{fl/+}; ROR α ^{Cre/+}) and cKO (COUP-TF1^{fl/fl}; ROR α ^{Cre/+}) cortices, as in the schematic at top left, processed using whole-mount in situ hybridization (WMISH) for Igfbp5, Cad8, and Lmo4. Igfbp5 expression specifically delineates V1; Cad8 and Lmo4 show lower expression in V1 and higher expression in V^{HO} and delineate both. These differential expression patterns in WT mice are lost in the cKO cortex and replaced with a uniform expression field that encompasses the entire occipital visual cortical field (marked with *). Scale bar, 0.5 mm.

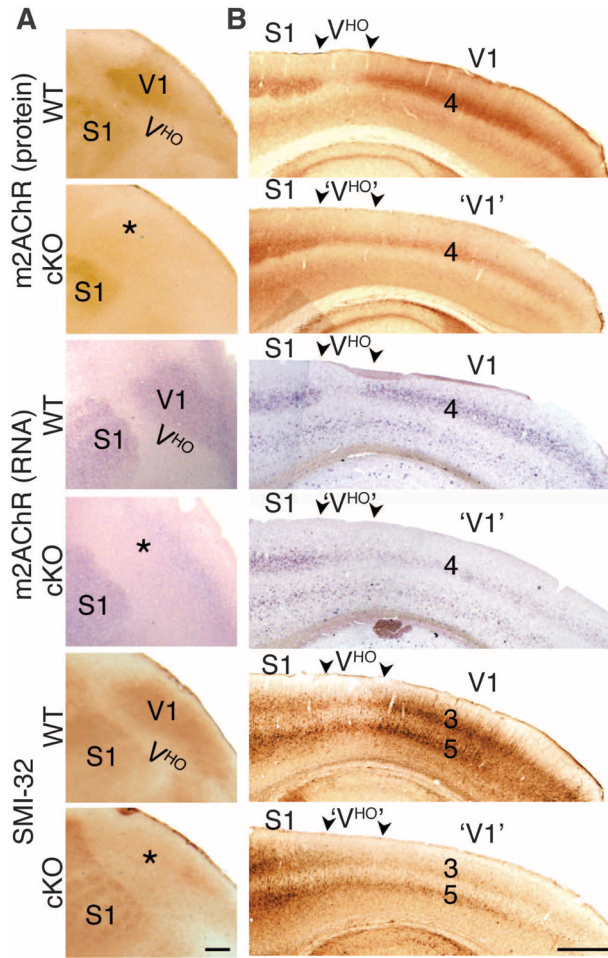


Fig. 4. Geniculocortical input drives differential patterning of genes and proteins that contribute to functional distinctions between V1 and V^{HO} in the adult cortex

Immunostaining for m2AChR and the SMI-32 epitope (a nonphosphorylated epitope on medium and heavy chains of neurofilaments that distinguishes functionally different forms) and ISH with an m2AChR probe on flattened tangential (A) and sagittal sections (B) of WT (COUP-TF1^{fl/+}; ROR α ^{Cre/+}) and cKO (COUP-TF1^{fl/fl}; ROR α ^{Cre/+}) cortices from adult (3-month-old) mice is shown. Rostral is to the left. In WT mice, m2AChR is highly expressed in layer 4 of V1, and SMI-32 is highly expressed in layers 3 and 5 of V1; both are expressed at low or nondetectable levels in V^{HO} of WT mice. In the cKO occipital cortex, m2AChR and SMI-32 are greatly down-regulated in V1 and modestly up-regulated in V^{HO}, resulting in uniform expression across the occipital visual cortical field (marked with *) posterior to S1 that would normally differentiate into V1 and V^{HO}. Scale bars, 0.5 mm.